I C A N S - V

MEETING OF THE INTERNATIONAL COLLABORATION ON

ADVANCED NEUTRON SOURCES

June 22-26, 1981

Gamma-ray measurements of isotopes produced by 1.1 GeV protons on lead and uranium targets

N.F. Peek, D.J. Shadoan and W. Amian*

University of California at Davis, California 95616, U.S.A.

* Institut für Reaktorentwicklung der KFA Jülich GmbH, Germany

Abstract

In order to simulate the spallation neutron source target, 3 cm diameter by 1 mm thick disks of Pb and U with Al monitoring foils and plates were irradiated at the Saturne National Laboratory at Saclay, France. The targets were embedded between 5 cm thick bricks (either natural Pb or depleted U). The overall target was 45 cm thick. In the case of the Pb experiment, 10 targets were included and for U, eight or nine. The study is progressing and has provided, so far, information on some 65 isotopes found in the 5 cm deep Pb target. Results are shown in the form of activities and atoms produced per incident proton. It will be possible to integrate the activities over all of the targets and estimate the isotope production, radioactive heat developed and, perhaps, the ensuing damage to the target materials.

Introduction

Development of a high flux neutron source utilizing the spallation reaction necessarily involves extensive study of residual activity produced in the target material. The majority of this activity arises via two mechanisms: a) high energy proton spallation reactions and the accompanying nuclear reactions from lower energy secondary particles produced during the spallation process and b) nuclear fission, i.e. fissioning of the high Z target material induced with particles from a high energy, high intensity proton irradiation. Equally important in spallation target design and optimization is isotope identification, isotope production rates and their spatial distribution throughout the target. Of interest are the possible target degrading elements which may, either from direct production or later via chemical reactions, be involved in excess gas production, corrosion or amalgamation in the target material.

Briefly, the experimental procedures involved irradiation of relatively thin, 1.0 mm thick, target foils embedded at equally spaced intervals in a larger target whose physical dimensions were similar to those of the proposed "infinitely thick" spallation target wheel. Two target materials were chosen for investigation, natural Pb and depleted U. An 1100 MeV proton beam with an average intensity of up to 80 nA was used for irradiations. Once irradiated the target foils were removed and counted using high resolution gamma-ray spectroscopy. The resulting data were recorded on magnetic tape for subsequent computer analysis and isotope identification. The inherent complexity of the data presented difficulties for complete analysis by computer and in most cases final values were confirmed before inclusion in this report. Many of the data have been compared to theoretical calculations from Monte Carlo transport codes and, in general, agree favorably /1/.

Experimental Procedures

a) High energy proton source

All irradiations for this experiment were conducted at Saturne National Laboratory within the Centre d'Etudes Nucléaires de Saclay located 25 km southwest of

Paris, France. The Saturne synchrotron provided proton beams of 600 MeV and 1100 MeV with average intensities of from 20 to 80 nA. Two quadrupole doublet magnets, upstream of the target area, provided strong focusing with resultant beam diameters at the target entrance between 1.0 and 1.5 cm FWHM. Small crossed-wire proportional chambers enabled the measurement of the horizontal and vertical profiles of the beam upstream and downstream from the target area before the insertion of the remotely controllable target blocked the beam from the downstream wire chamber. Figures 1 and 2 show, in general, a Gaussian intensity distribution for both vertical and horizontal beam profiles. The beam spot was nearly circular. The beam position was monitored continuously throughout each irradiation with the upstream wire chamber.

b) Target configuration

Two target materials were investigated during this research, natural Pb and depleted U. For both materials the gross features of the total target, target foil assembly were kept as nearly identical as possible. Figure 3 shows the configuration of the Pb target in detail. The first target foil shown was an aluminum foil (3.0 cm diameter by 1.0 mm thick) positioned 5.0 cm in front of the main target assembly. In this position it was utilized to monitor the incoming proton intensity by a method discussed later in this section. The next target foil (the first Pb foil) was positioned directly in front of the main assembly to receive full beam energy. Immediately behind the first Pb foil followed a 1.0 mm thick aluminum plate scribed with lines forming a grid with 1.0 cm divisions used to monitor the beam distribution (Figs. 1 and 2) (i.e. vertical and horizontal intensity profiles), in the same manner as the first aluminum target foil. The three target elements described above, Al foil, Pb foil, and Al plate, constituted a repetitive unit and appeared a total of 10 times; each unit separated by a 5.0 cm thick Pb brick. Individual target foils consisted of 3.0 cm diameter by 1.0 mm thick natural Pb disks. These dimensions were chosen as a compromise between adequate counting intensity and corrections due to self-absorption and non point-source geometry. Due to space limitations in the target area the total length, 45 cm, of the complete Pb target assembly was short of the "infinite thickness", 65 cm, required to completely absorb 1100 MeV protons. Stopping-power calculations indicated an energy loss of 700 MeV in 45 cm of Pb.

The uranium target, target foil assembly was identical except for two instances. First, the entire target assembly was infinitely thick at an overall length of only 35 cm and therefore the number of uranium target foils irradiated was eight in one run and nine in the next. Secondly, the uranium foils were vacuum encapsulated in aluminum cases to prevent the escaping of radioactive gases.

c) Beam intensity monitoring

Aluminum activation provided an excellent method for determining beam particle intensity via the reactions listed in Table 1. This table shows the possible modes of production of three isotopes from an Al target namely ^{24}Na, ^{22}Na and ^{7}Be. Also included are the calculated Q-values for each reaction and the production cross-sections at spallation energies as well as at lower energies where compound nuclear reactions dominate. The large differences in Q-values between the sodium isotopes and beryllium-7 provided some information on the secondary particle energy distribution throughout the target. The lower energy secondary particles produced less ^{7}Be due to the 190 MeV Q-value. As previously described, each Pb and U target foil was preceeded by an aluminum beam-monitoring foil of the same diameter and thickness. Data from these foils provided incident intensity normalizations for activity calculations for both Pb and U target foils. After the initial target, beam particles were no longer distinguishable as primary beam protons but contained, in addition, scattered protons and neutrons from spallation. Following each target foil an aluminum plate, 10 x 20 x 0.1 cm, was used to establish the beam particle distribution as a function of depth into the target. The beam profile plates were analyzed for Na isotopes and ^{7}Be by scanning an area of 1 cm^2 in 1 cm steps over the rectangular coordinate system scribed on the plates. The data points were plotted and fitted mathematically with a Gaussian distribution and the results are shown in figures 1 and 2. The position of the beam with respect to the monitor foil was determined by this technique and integration over the target area produced the percentage and intensity of the beam that struck the target. (Note that the beam in this run was about 0.1 cm to the right and about 1.1 cm low). The shape of the beam became broader and less intense, with depth into the target (see figure 4). The parameters for the construction of figure 4 are found in table 2.

d) Data collection

The data collection system included, besides normal high resolution gamma-ray counting electronics, a multichannel analyzer controlled automatic sample changer (Fig. 5). The 80 cm^3 Ge(Li) detector, pulse amplifier and shaping electronics and 100 MHz ADC, all Canberra products, had an energy resolution of 2.0 KeV at 1.0 MeV and 5000 c/sec. The microprocessor controlled multichannel analyzer, also from Canberra, was keyboard programmable to collect, record and partially analyze gamma-ray data from two simultaneously operating detector systems. After data from each target foil was collected the analyzer sequenced the automatic sample changer and the next target foil was counted. The capacity of the sample changer was 16 foils. Although the analyzer contained "dead time" accounting electronics a 50 MHz precision pulser was used to calculate any dead time not compensated for by the analyzer. The counting system showed negligible gain shift and line broadening up to 30,000 c/sec. IAEA and PTB standard reference sources with ± 2% accuracy were used for absolute calibration. The automatic sample changer with a capacity of 16 samples was mounted on rails and could be easily positioned at different distances from the detector to maximize data acquisition rates to the Ge(Li) system. Both the detector and target wheel assembly were enclosed in Pb shielding 10 cm thick. Target foil and detector geometries were defined by 5.0 cm diameter openings in each enclosure. Counting of irradiated target foils began at Saturne in Saclay 30 minutes after end of irradiation and continued after 6 days at KFA in Jülich on a similar detector system. (In order to count at close distances at Jülich, the target wheel was not shielded and contained only four sources). The counting time interval was calculated by dividing the elapsed time since end of irradiation by 5 (this would be an isotope half-life whose activity had decreased by a factor of 32) and counting for 10% of that time. In this manner, the error made by assuming a linear decay over the counting interval is less than 1%.

Data Reduction

Computer analysis and reduction was performed primarily in two main stages. Initially, all data were translated and transferred to an IBM 370 from the

analyzer created magnetic tapes and a gamma-ray fitting procedure, AGAMEMNON, provided all gamma-ray intensities as a function of energy. Finally, a sorting and isotope identification procedure produced output as a function of energy and time-since-end of irradiation for each target foil. During both stages of analyses software modifications were required in order to accomodate the enormous number of gamma-rays emitted by each target foil (see Fig 6 and 7). Each spectrum contained no less than 150 identifiable gamma-rays (maximums of over 300 were common). At short times after irradiation gamma-rays were so numerous that a high background was generated, making it difficult to identify isotopes.

During the initial translation and transfer of data, all additional relevant parameters required for analysis were included in the data set. These parameters included elapsed time since the end-of-irradiation, target foil counting geometry and target foil identifiers. The resulting data became input to AGAMEMNON which processed an average of 30 spectra per hour of CPU time. This computer code takes the prepared spectral input from disc and processes each spectrum individually to determine the energy that corresponds to the centroid and the area of all peaks above a controllable significance level. The code outputs this information as a disc file for the half-life analysis, and as paper output of the fit obtained for each peak.

AGAMEMNON offers a variety of fitting options: Internal or external lineshape calibration, Gaussian on a smoothly varying background or Gaussian with exponential tail and optional stepfunction under strong peaks /2, 3/. Goodness-of-fit criteria are χ^2_r and RMS /4/ for the fitted region and FOM /5/ for the peak region and the background region individually.

The resolution of multiplets is performed by the peak locating algorithm a method of convolution with a zero-area Gaussian /6/. This algorithm is applied to the original spectrum and, in cases where the goodness-of-fit criteria are not reached, updated peakshape parameters for the region under consideration and the residual spectrum are allowed to vary to decide if an additional peak has to be considered. The output from AGAMEMNON, line energies and intensities, was collected for each individual target foil and the subsequent data array

was ordered with increasing time since end of irradiation. From these data all gamma-rays with energies from 120 KeV to 2000 KeV were sorted into energy groups with a maximum allowable deviation of 2.0 KeV. In this manner, all gamma-ray intensities from each target foil were cataloged by increasing time since end of irradiation thereby allowing decay curves to be plotted for each energy.

Initial isotope identification was made from a search of gamma-ray energies from Erdtmann and Soyka /7/ and the Table of Isotopes /8/ and choosing only those which match with isotopes having gamma-rays within ± 2.0 KeV of the energy of the line plotted on the decay curves. The best combination of isotopes which fitted the decay curve was selected as the constituent isotopes for a particular target foil and energy. Once preliminary identification was made parent daughter relationships for these isotopes were investigated and total activity reported as cummulative i.e.

$$A_c = A_d + A_{pd}$$

where A_d = Activity directly made

A_{pd} = Activity from parent-daughter decay

In the case of Bi isotopes and most metastable (high ground state spin) isotopes, direct made activities were calculated (table 3).

Discussion

The nature of isotope counting dictates that counting continue over a period of several months. This is especially true if the number of isotopes is very large such as in the case of spallation reactions. For isotope production with 100 MeV protons, it is expected that one gamma line in 10 will be a doublet. However, with isotopes produced by 1100 MeV protons approximately 7 out of 10 gamma lines are multiplets (Figs. 6, 7). Therefore, counting must continue for an extended period in order to unfold the half-lives and identify each isotope. Considering these facts it is reasonable that the data presented are preliminary.

Table 3 presents the isotopes found thus far in the target foil Pb 2. The distinction has been made between direct and cumulative production for these isotopes. The cumulative isotopes represent a parent-daughter cascade in the direction of the stability curve and the activities are given at a time when the daughter growth was a maximum, (t_{max}). In all cases, the cumulative isotopes column includes the direct made portion. Table 3 includes possible induced fission products. They are listed in the "direct made" column. With these data it is possible to calculate the number of atoms of a particular isotope produced per incoming proton per g/cm^2 thickness of the target foil. By gathering similar information from the other 9 targets (in the case of the Pb target) it will be possible to calculate the amount of each isotope produced in the total target assembly by integrating over the pathlength of the beam.

Figure 8 shows a comparison between the radiation power generated by the gamma-rays in the decay of the U and Pb targets. These data are from the second target foil at a depth of 5.0 cm into the target assembly. The data points were calculated by integrating the gamma radiation from 100 KeV to 2000 KeV in 100 KeV steps, and folding in the efficiency of the detector. The power is given as Watts per incoming proton per g/cm^2 thickness and, as shown, approximately 5 times more power was generated from the U target foil than from the Pb target foil. It is interesting to note from the figure that the two curves cross at about 1700 KeV. This behavior is explained by the fact that the activities produced by U have many more low energy gamma-rays than Pb and comparatively less at high energy.

Figures 1 and 2 are calculated from the production of ^{24}Na by the beam at two locations in the Pb target. Sodium-24 with its higher cross-section for lower energy protons and neutrons is more likely to indicate the presence of lower energy secondary particles, along with the primary high energy beam (Table 1). Sodium-22 and particularly ^{7}Be would show the distribution of the higher energy beam particles in the target assembly. The combination of these data help provide information on the energy distribution of the beam particles throughout the total target. It is interesting to note that the peak flux from the second plate at 5 cm depth into the main target is about 25 times higher than the peak flux at 40 cm. When comparing total intensity only one order of magnitude

difference appeared, due to beam spreading (Fig. 4). When the same comparisons are made between ^{7}Be and ^{22}Na the results should indicate that the ^{7}Be has a much narrower distribution more representative of the high energy proton beam.

At this writing a phenominally large amount of data has been collected and partially analyzed. The outlook for accurate and repeatable results is very good. There have been two successful accelerator irradiations, of both the Pb and U targets, with adequate beam intensity to provide sufficient activation of the target foils. Data collection and analysis will continue over the next year and final results will be more complete at that time.

References

/1/ T.W. Armstrong,
Realisierungstudie zur Spallations-Neutronenquelle
Vol. 2, A 2.6 (1981)

/2/ J.W. Phillips, et al.
Nucl. Inst. + Meth. 153 (1978) 449

/3/ L.A. McNelles et al.
Nucl. Inst. + Meth. 127 (1975) 73

/4/ T. Sehine et al.
Nucl. Inst. + Meth. 133 (1976) 171

/5/ H.I. Balian et al.
Nucl. Inst. + Meth. 145 (1977) 389

/6/ I. De Lotto et al.
Nucl. Inst. + Meth. 143 (1977) 617

/7/ G. Erdtmann, W. Soyka
The Gamma Rays of the Radionuclides, Vol. 7
Verlag Chemie, Weinheim-New York, 1979

/8/ C.M. Lederer, V.S. Shirley
Table of Isotopes, 7th Edition, John Wiley + Sons Inc. New York 1978

/9/ N.F. Peek, F. Hegedüs
The Production of Xenon Isotopes with Protons of Energies from 320 to 590 MeV
Int. J. of Applied Rad. + Isotopes, 30 (1979) 661-635

Reaction	Q(MeV)	Spallation σ(mb) at 1.1 GeV	Nuclear σ_{max}(mb) at E(MeV)
^{27}Al (p,x) ^{24}Na		11	11 80
x = 3 p,n	-31		
x = p,d	-20		
^{27}Al (n,α) ^{24}Na	- 3	-	129 13
^{27}Al (p,x) ^{22}Na		15	40 45
x = 3p,3n	-50		
x = α,d	-20		
^{27}Al (n,x) ^{22}Na			
x = 2p,4n	-51		
x = α,2n	-23		
^{27}Al (p,x) ^{7}Be		8	1 80
x = 10p,11n	-190		
x = 5α,n	- 46		
^{27}Al (n,x) ^{7}Be			
x = 9p,12n	-190		
x = 4α,d,3n	- 72		

Table 1 Aluminum Monitor Foil Reactions /9/

target	depth (cm)	μ_{vert} (cm)	FWHM (Γ cm)	Intensity (c/sec)	% on target
1	0	-1.24	1.3	255	81
2	5	-1.13	1.8	230	80
3	10	-1.06	2.4	172	76
4	15	- .97	3.2	100	67
5	20	- .89	4.3	58	56
6	25	- .80	5.8	33	45
7	30	- .73	7.9	19	34
8	35	- .62	10.6	11	28
9	40	- .54	14.4	6.2	19
10	45	- .46	19.4	4.6	15

(μ_{horiz} = + .095 cm)

Table 2 Beam Parameters from ^{24}Na Measurements for the Series Pb 51 Targets

Isotope	T1/2	Direct made Activity (d/sec; $\Delta t_{EOB} = 0$) $\cdot 10^5$	Cumulative Activity (d/sec; $\Delta t_{EOB} = t_{max}$) $\cdot 10^5$	(Atoms/g/cm^2/H$^+$) $\cdot 10^{-5}$
^{202}Bi	1.67 h	22.		1.3
^{203}Bi	11.8 h	4.8		2.0
^{204}Bi	11.3 h	6.9		2.8
^{205}Bi	15.3 d	0.25		3.3
^{206}Bi	6.2 d	0.42		2.2
^{197M}Pb	42. m	370.		9.2
^{198}Pb	2.4 h		60. at 0.8 h	5.1
^{199}Pb	1.5 h		30. at 1.1 h	1.6
^{200}Pb	21.5 h		15. at 3.1 h	11.4
^{201}Pb	9.4 h		50. at 5.0 h	16.7
^{202M}Pb	3.6 h	30.		3.8
^{203}Pb	52.1 h		6.3 at 32.7 h	11.6
^{204M}Pb	1.15 h	110.		4.5
^{194M}Tl	33. m	48.		0.94
^{196}Tl	5.3 h		35, at 5.0 h	6.6
^{198M}Tl	1.87 h	97.		6.4
^{199}Tl	7.4 h		23. at 4.3 h	6.0
^{200}Tl	26.1 h		6.6 at 34.1 h	6.1
^{201}Tl	73.5 h		3.8 at 31.9 h	9.9
^{202M}Tl	12.2 d		.48 at 23.2 h	5.0
^{192}Hg	4.9 h		25.9 at 0.84 h	4.5
^{193M}Hg	11.1 h	5.8		2.3
^{195M}Hg	1.7 d	2.2		3.2
^{197M}Hg	23.8 h	0.28		0.24
^{199M}Hg	42.6 m	31.		0.78
^{190}Au	42.8 m		120. at 40.8 min	3.0
^{192}Au	5.0 h		8.7 at 7.1 h	1.5
^{193}Au	17.6 h		11. at 10.2 h	6.9
^{194}Au	39.5 h	0.96		1.3
^{196}Au	6.17 d	0.15		0.79
^{196M}Au	9.7 h	16		5.5
^{198}Au	2.7 d	0.30		0.69
^{198M}Au	2.3 d	0.21		0.41
^{200M}Au	18.7	0.46		0.31
^{188}Pt	10.3 d		0.67 at 1.6 h	5.9
^{189}Pt	10.9 h		37. at 2.3 h	14.3
^{191}Pt	2.8 d		2.6 at 14.8 h	6.2
^{195M}Pt	4.1 d	1.3		4.5
^{184}Ir	3.0 h		23. at 1.1 h	2.4
^{186}Ir	15.8 h		3.4 at 6.8 h	1.9
^{187}Ir	10.5 h		23. at 6.5 h	8.6
^{188}Ir	41.4 h		0.7 at 128. h	1.0
^{190}Ir	12.2 d	0.03		
^{182}Os	21.8 h		7.8 at 1.6 h	6.0
^{185}Os	94. d		0.076 at 104. h	6.1
^{182M}Os	2.7 d	0.66		1.5
^{178M}Ta	2.2 h	77.		6.0
^{173}Hf	23.6 h		30. at 11.5 h	25.1
^{169}Lu	1.4 d		2.4 at 0.5 h	2.9
^{171}Lu	8.2 d		0.47 at 52.3 h	3.3
^{169}Yb	32.0 d		0.15 at 1.3 h	4.1
^{160}Er	28.6 h		0.95 at 1.2 h	0.96
^{147}Gd*	38.0 h	17.		22.9
^{149}Gd*	9.3 d	.07		0.55
^{146}Eu*	48.3 d	0.5		20.5
^{148}Eu*	54.5 d	0.65		30.2
^{128}Ba*	2.42 d	0.97		2.0
^{89M}Zr*	78.5 h	0.14		0.39
^{87}Y*	80.3 h	0.20		0.57
^{83}Rb*	68.2 d	0.008		0.59
^{74}As*	17.8 d	.02		0.30

* Possible Fission Fragments

Table 3 Isotope Production of the Second Pb Target (5 cm deep)

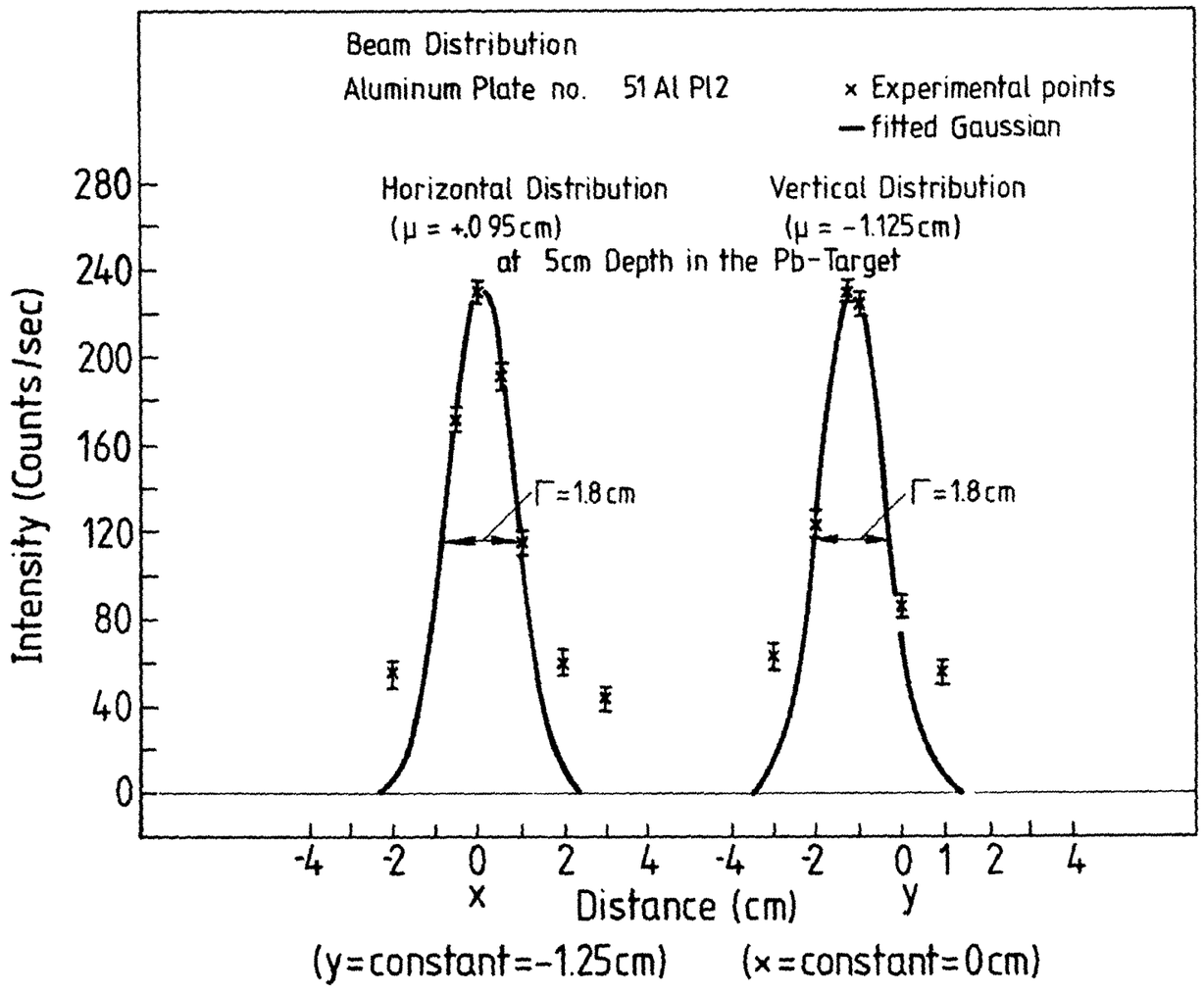

Fig. 1 Beam distribution 5 cm deep in the Pb target produced from induced ^{24}Na activity measurements in an aluminum plate (10 x 20 x 0.1 cm)

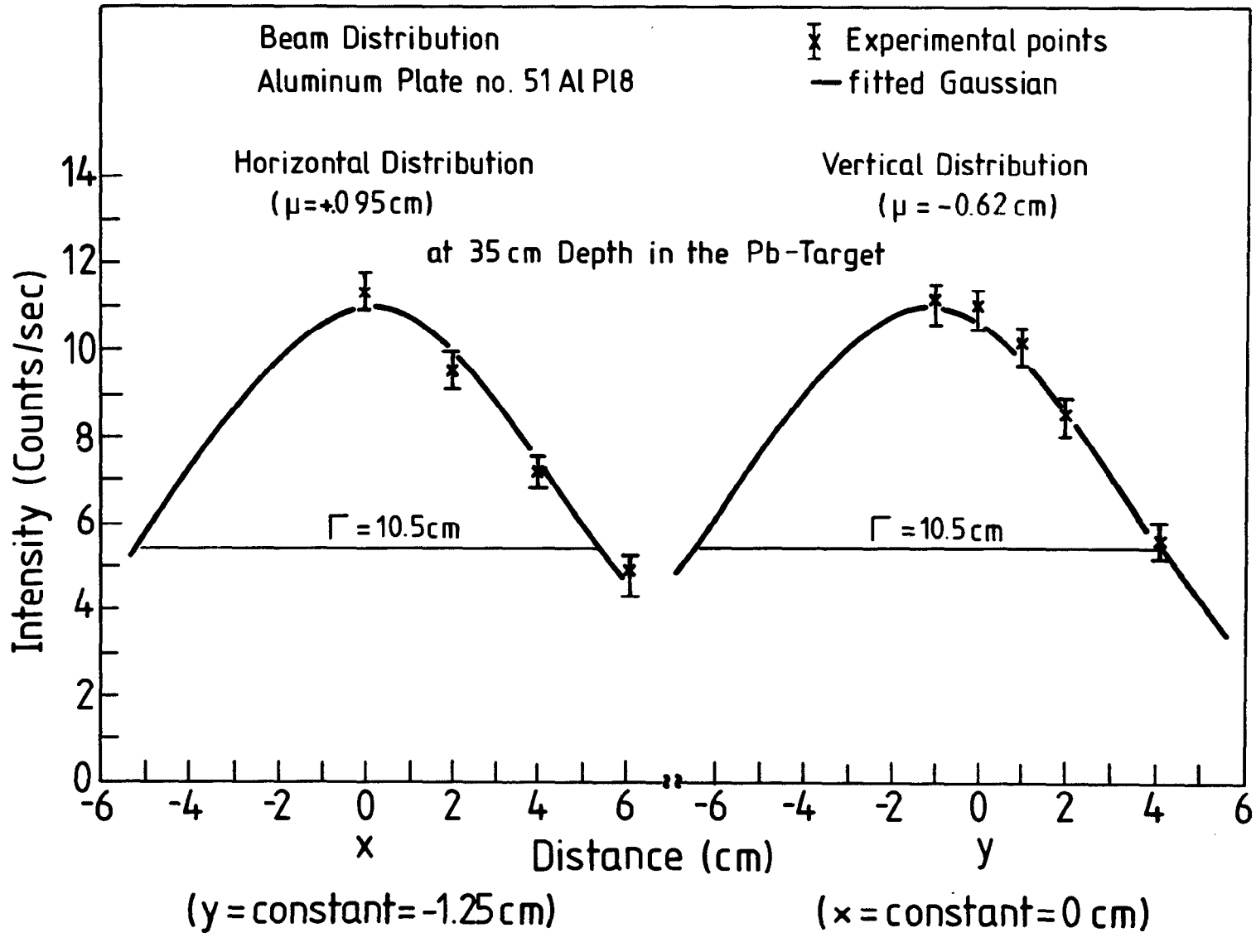

Fig. 2 Beam distribution 35 cm deep in the Pb target produced from induced ^{24}Na activity measurements in an aluminum plate (10 x 20 x 0.1 cm)

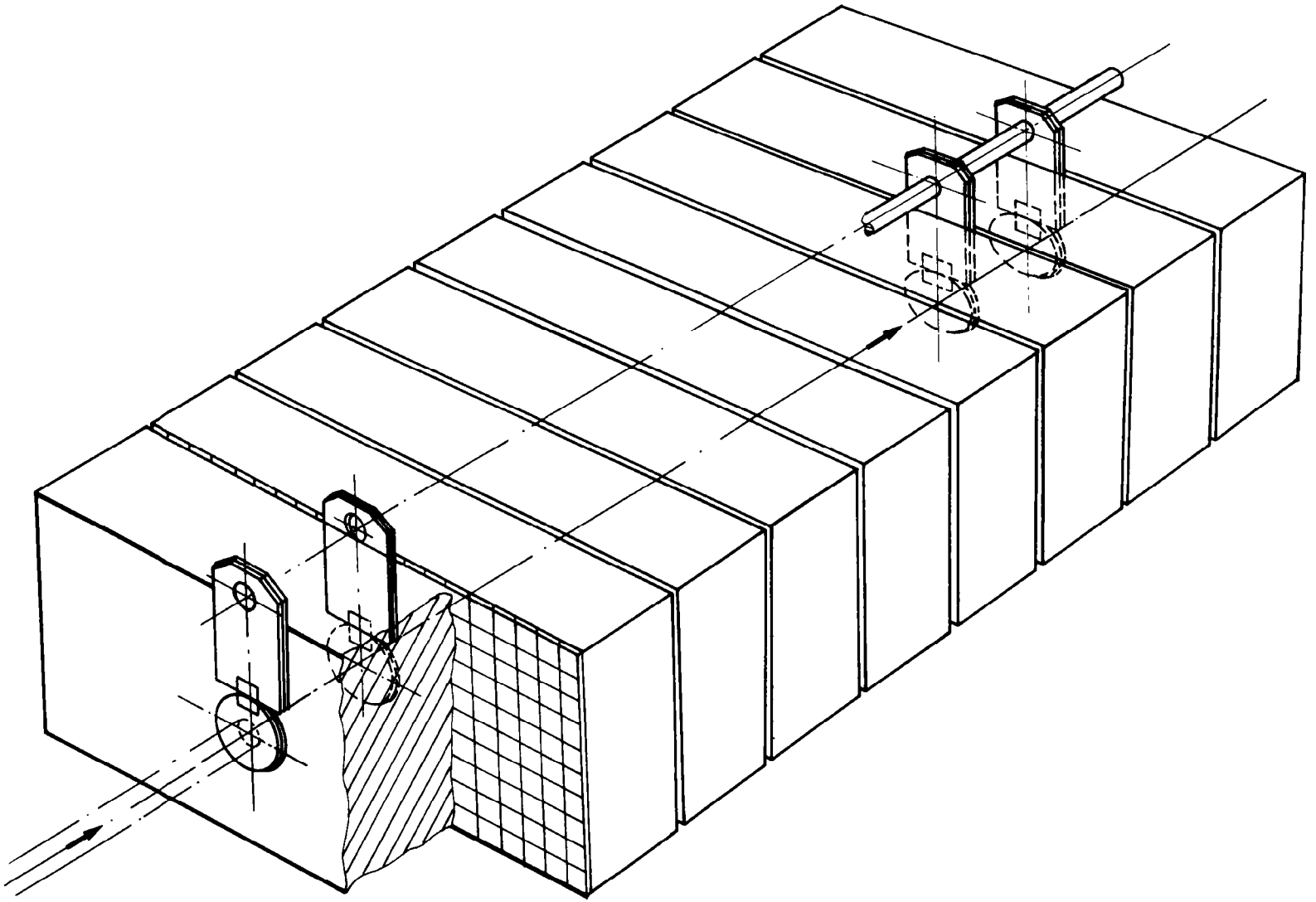

Fig. 3 Target configuration showing the small target disk followed by an aluminum disk and an aluminum plate along with the 5 cm thick Pb brick.

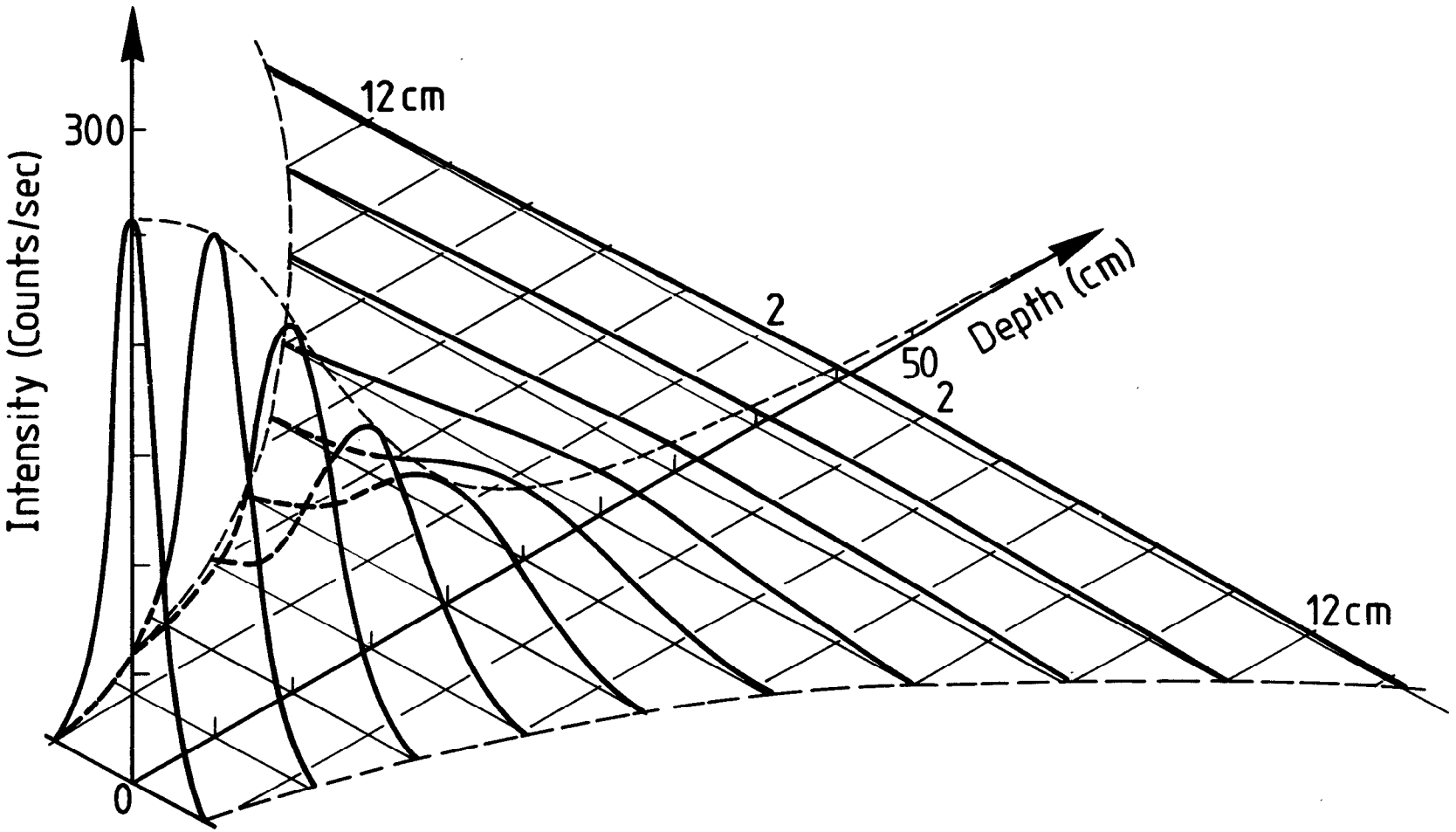

Fig. 4 Overall beam distribution on a function of depth constructed from ^{24}Na measurements of the 10 Al plates from the Pb target

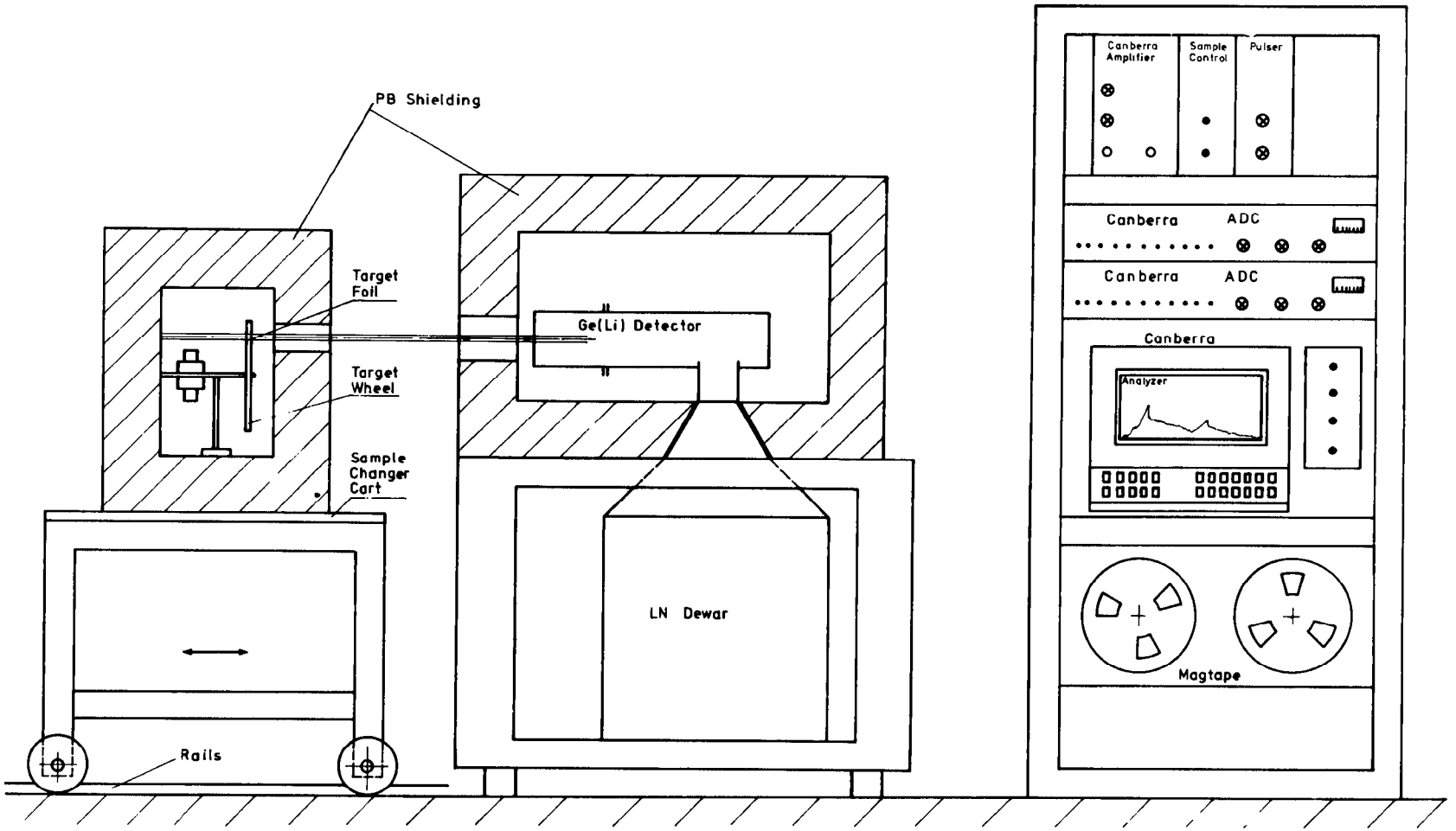

Fig. 5 Schematic of the radioactive counting equipment

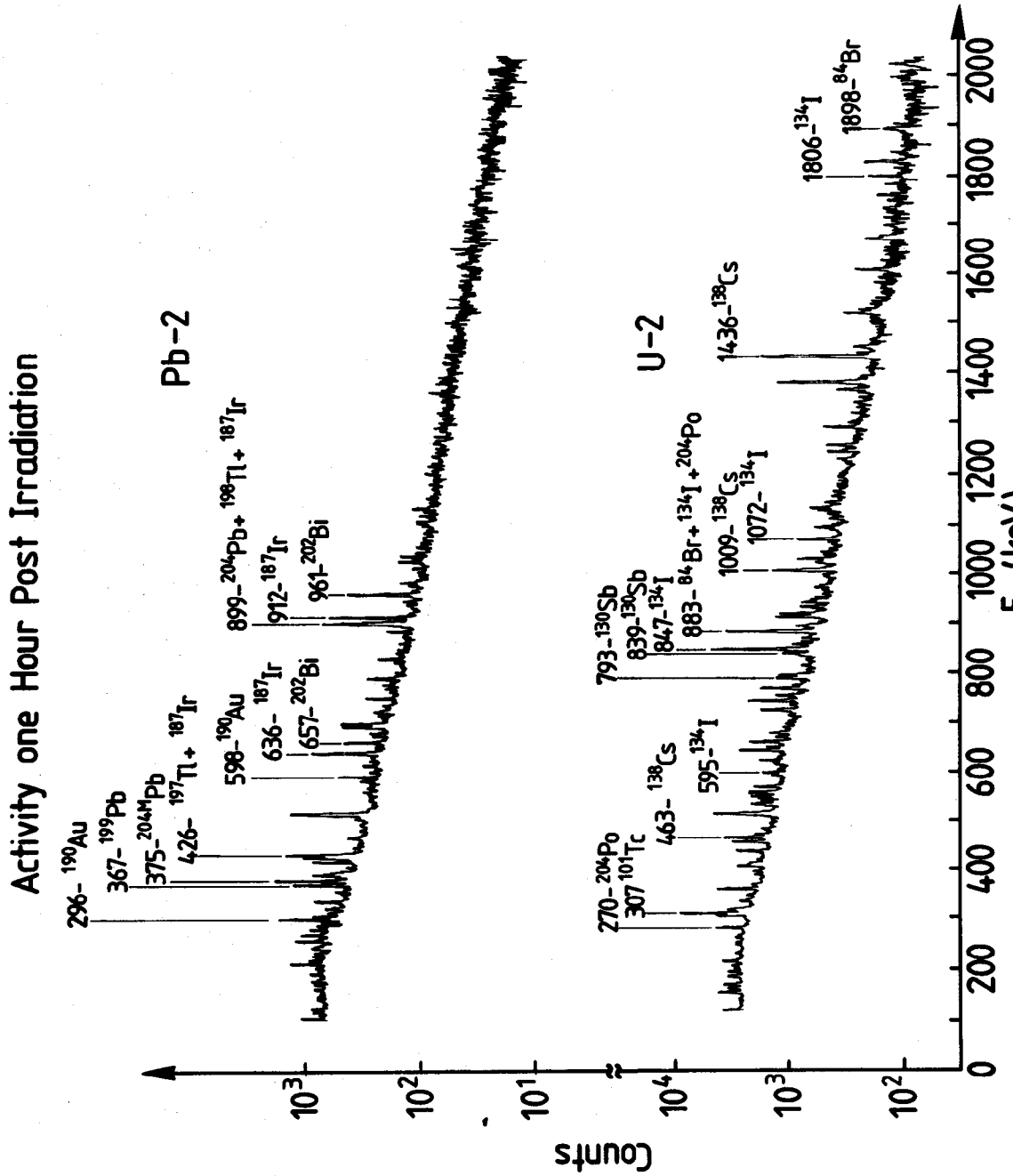

Fig. 6 Spectra from both Pb and U targets which were 5 cm deep in the over-all target taken on hour after the bombardment

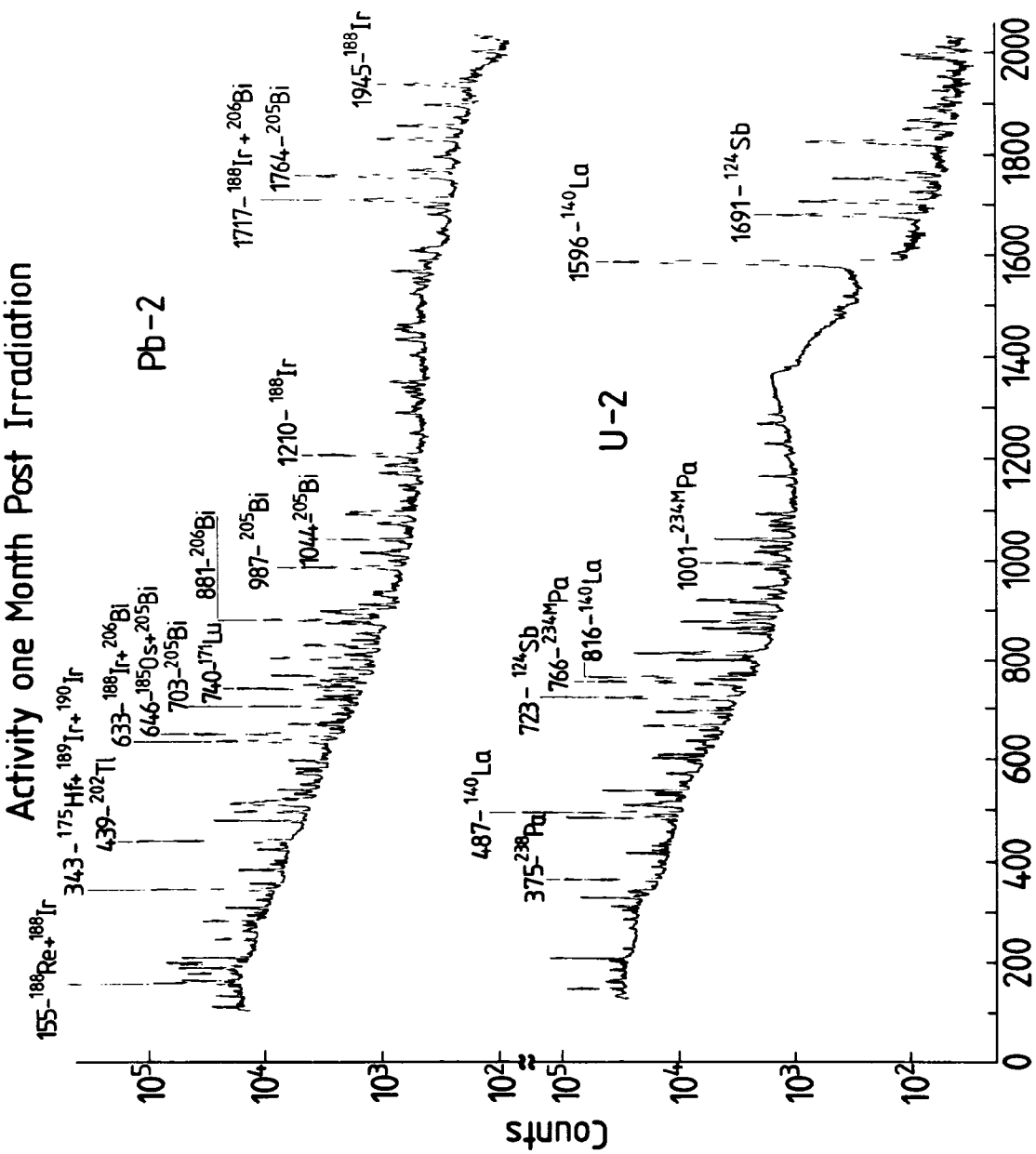

Fig. 7 Spectra from both Pb and U targets which were 5 cm deep in the over-all target taken one month after the bombardment

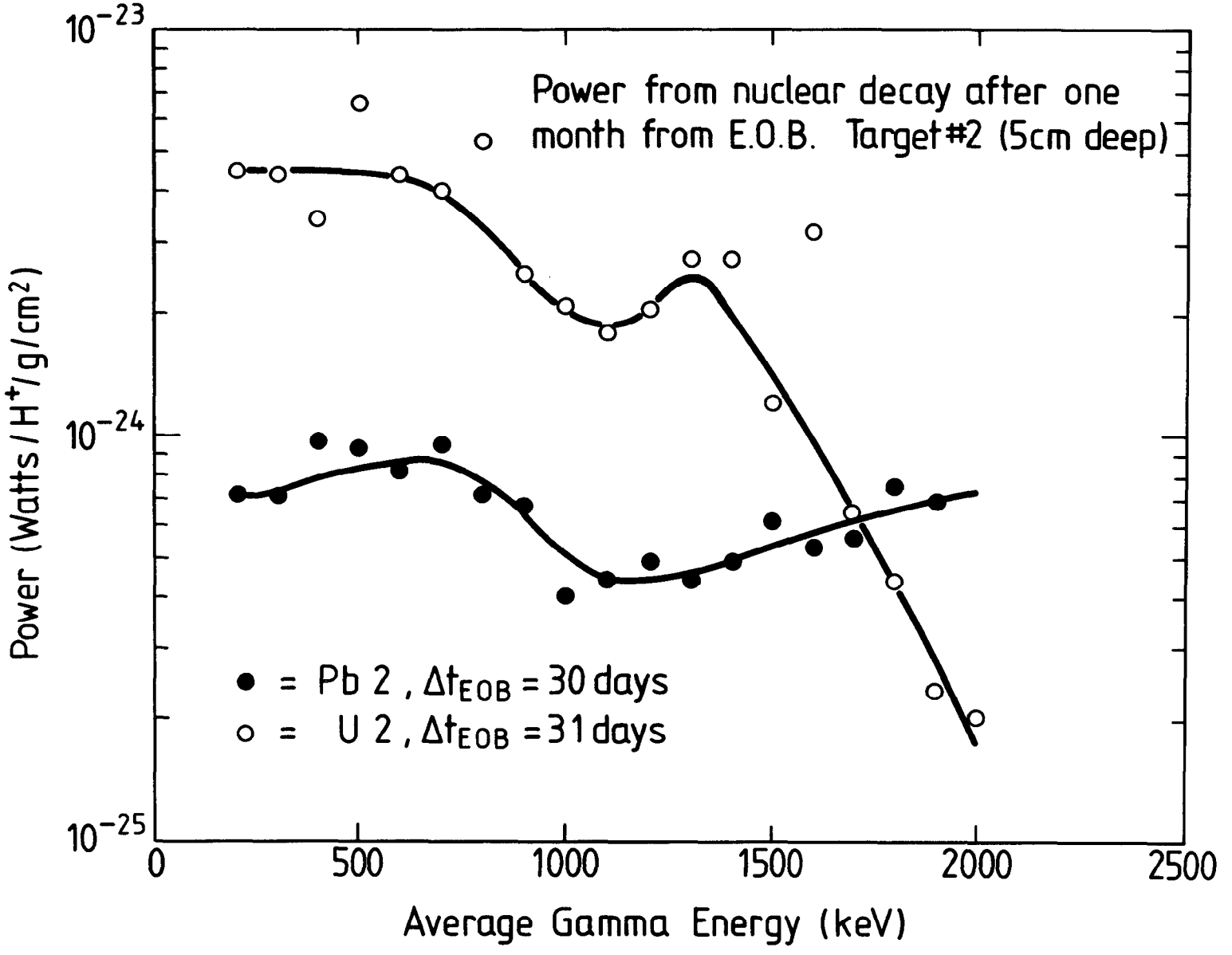

Fig. 8 Radiation power generated by the gamma rays from the decay of the U and Pb targets 5 cm deep into the over-all targets